

# Enhanced dual function of osteoclast precursors following calvarial *Porphyromonas gingivalis* infection

Xia Cai<sup>1,2</sup> | Zhaofei Li<sup>1,3</sup> | Yanfang Zhao<sup>1</sup> | Jenny Katz<sup>1</sup> | Suzanne M. Michalek<sup>4</sup> |  
Xu Feng<sup>5</sup> | Yuhong Li<sup>3</sup> | Ping Zhang<sup>1</sup> 

<sup>1</sup>Department of Pediatric Dentistry, School of Dentistry, University of Alabama at Birmingham, Birmingham, AL, USA

<sup>2</sup>Department of Periodontics, The Affiliated Stomatological Hospital, School of Medicine, Zhejiang University, Hangzhou, China

<sup>3</sup>Department of Endodontics, School of Stomatology, Wuhan University, Wuhan, China

<sup>4</sup>Department of Microbiology, University of Alabama at Birmingham, Birmingham, AL, USA

<sup>5</sup>Department of Molecular & Cellular Pathology, School of Medicine, University of Alabama at Birmingham, Birmingham, AL, USA

## Correspondence

Ping Zhang, Department of Pediatric Dentistry, School of Dentistry, University of Alabama at Birmingham, Birmingham, AL, USA.

Email: pingz@uab.edu

Yuhong Li, Department of Endodontics, School of Stomatology, Wuhan University, Wuhan, Hubei, China.

Email: 1004809372@whu.edu.cn

## Funding information

National Institute of Dental and Craniofacial Research, Grant/Award Number: DE022401, DE026465 and DE022736; National Institutes of Health, Grant/Award Number: P30AI27667, P30AR048311, P30DK056336, P30DK079626 and P30AG050886A

## Abstract

**Background and objective:** Excessive osteoclast activity is a major characteristic of pathogenic bone loss in inflammatory bone diseases including periodontitis. However, beyond the knowledge that osteoclasts are differentiated from the monocyte/macrophage lineage and share common ancestry with macrophages and DC, the nature and function of osteoclast precursors are not completely understood. Furthermore, little is known about how osteoclast precursors respond to bacterial infection in vivo. We have previously demonstrated in vitro that the periodontal pathogen *Porphyromonas gingivalis* (*Pg*) plays a biphasic role on the receptor activator of nuclear factor kappa B ligand (RANKL)-induced osteoclast differentiation. In this study, we investigated the in vivo effect of *Pg* infection on the regulation of osteoclast precursors, using a mouse calvarial infection model.

**Methods and results:** C57BL/6 wild-type and the myeloid differentiation factor 88 knockout (*MyD88*<sup>-/-</sup>) mice were infected with *Pg* by calvarial injection. Local and systemic bone loss, and the number and function of CD11b<sup>+</sup>c-fms<sup>+</sup> cells from bone marrow and spleen were analyzed. Our results show that *Pg* infection induces localized inflammatory infiltration and osteoclastogenesis, as well as increased number and osteoclastogenic potential of CD11b<sup>+</sup>c-fms<sup>+</sup> osteoclast precursors in the bone marrow and periphery. We also show that CD11b<sup>+</sup>c-fms<sup>+</sup>RANK<sup>+</sup> and CD11b<sup>+</sup>c-fms<sup>+</sup>RANK<sup>-</sup> are precursors with similar osteoclastogenic and pro-inflammatory potentials. In addition, CD11b<sup>+</sup>c-fms<sup>+</sup> cells exhibit an antigen-specific T-cell immune-suppressive activity, which are increased with *Pg* infection. Moreover, we demonstrate that *MyD88* is involved in the regulation of osteoclast precursors upon *Pg* infection.

**Conclusions:** In this study, we demonstrate an enhanced dual function of osteoclast precursors following calvarial *Pg* infection. Based on our findings, we propose the following model: *Pg* infection increases a pool of precursor cells that can be shunted toward osteoclast formation at the infection/inflammation sites, while at the same time dampening host immune responses, which is beneficial for the persistence of infection and maintenance of the characteristic chronic nature of periodontitis. Understanding the nature, function, and regulation of osteoclast precursors will be

This is an open access article under the terms of the Creative Commons Attribution-NonCommercial License, which permits use, distribution and reproduction in any medium, provided the original work is properly cited and is not used for commercial purposes.

© 2020 The Authors. *Journal of Periodontal Research* Published by John Wiley & Sons Ltd.

helpful for identifying therapeutic interventions to aid in the control and prevention of inflammatory bone loss diseases including periodontitis.

#### KEYWORDS

bone loss, MyD88, osteoclast precursors, *Porphyromonas gingivalis*

## 1 | INTRODUCTION

Osteoclasts are multinucleated giant cells that resorb bone, ensuring development and continuous remodeling of the skeleton and the bone marrow hematopoietic niche.<sup>1</sup> Excessive activity of osteoclasts is a characteristic feature of pathogenic bone loss in osteolytic diseases including periodontitis and rheumatoid arthritis.<sup>2,3</sup> It is believed that osteoclasts are derived from hematopoietic stem cells (HSC) of the monocyte/macrophage lineage—the common precursors for macrophages and dendritic cells (DC)—that undergo several key differentiation stages, including the differentiation of common myeloid progenitors and granulocyte/macrophage progenitors.<sup>4,5</sup> Most recently, it is suggested that osteoclasts may originate from the embryonic erythro-myeloid progenitors and that HSC-derived precursors cells are important for optimal postnatal osteoclast maintenance and function.<sup>1</sup> Regardless of the origin, osteoclast differentiation requires the presence of two essential molecules: the macrophage colony-stimulating factor (M-CSF) and the receptor activator of nuclear factor kappa B ligand (RANKL).<sup>5,6</sup> While M-CSF primarily promotes the proliferation and survival of osteoclast progenitors via its receptor c-fms, RANKL prompts the cells to differentiate along the osteoclast lineage by binding to its receptor RANK, expressed on osteoclast precursors and mature osteoclasts.

Periodontitis, a chronic, infectious, inflammatory disorder characterized by the loss of alveolar bone, is one of the most common human infectious diseases and the primary cause of tooth loss in adults.<sup>7</sup> *Porphyromonas gingivalis* (*Pg*) is considered a major etiologic agent of periodontitis and has been closely associated with the inflammatory destruction of alveolar bone. While the presence of pathogenic bacteria and inflammation are prerequisites for periodontal bone loss, the precise mechanisms underlying host susceptibility to periodontitis, maintenance of chronic inflammation, and triggering of alveolar bone resorption are still not clearly understood. For instance, it is unclear why some individuals have periodontal pathogens in their periodontium without manifesting the disease,<sup>8-10</sup> and why untreated gingivitis does not always result in periodontitis.<sup>11,12</sup>

It is generally accepted that pathogenic osteoclast formation in periodontitis involves several major mechanisms: (a) periodontal pathogens upregulate RANKL expression on osteoblasts and activated immune cells such as T cells and B cells, which stimulate the differentiation of osteoclast precursors into mature osteoclasts resulting in excessive bone loss<sup>13-15</sup>; (b) periodontal pathogens induce the production of inflammatory cytokines, such as TNF- $\alpha$  and IL-1, which synergize with RANKL and augment RANKL-mediated osteoclastogenesis<sup>16-18</sup>; and (c) periodontal pathogens potentiate RANKL-committed

osteoclast precursor differentiation into osteoclasts.<sup>19</sup> While these findings have demonstrated the important role of pathogenic bacteria and inflammatory cytokines in osteoclast formation from osteoclast precursors, it remains unclear how osteoclast precursors respond to periodontal pathogen infection in vivo and the role of osteoclast precursors in the pathogenesis of periodontal bone loss.

We have previously demonstrated in vitro that osteoclast precursors have two fates.<sup>19</sup> They function as inflammatory cells in response to *Pg* infection, or they differentiate into osteoclasts upon RANKL stimulation. Once a fate is chosen, it is irreversible. Importantly, the effect of *Pg* on cell fate determination dominates over that of RANKL. On the other hand, *Pg* potentiates osteoclastogenesis of RANKL-primed osteoclast precursors. It is likely that this biphasic role of *Pg* on osteoclast differentiation is important for the pathogenic consequences of periodontal infection. In this regard, soon after *Pg* invasion of periodontal tissues, *Pg* suppresses osteoclast precursor differentiation down the osteoclast pathway, while promoting an inflammatory response aimed at eradicating the invading pathogens. If the host cannot clear the infection efficiently and the infection persists, RANKL produced by activated immune and residential cells then primes circulating osteoclast precursors and stimulates osteoclastogenesis.

In this study, we further investigated the in vivo effect of *Pg* infection on the regulation of osteoclast precursors, using a mouse calvarial infection model. We found that *Pg* infection increased the percentage and the osteoclastogenic potential of CD11b<sup>+</sup>c-fms<sup>+</sup> precursor cells in bone marrow and periphery. In addition, these precursor cells exhibited antigen-specific T-cell suppressive function and *Pg* infection increased the immune-suppressive function of the cells. Furthermore, we showed the involvement of the myeloid differentiation factor 88 (MyD88) in the regulation of osteoclast precursors upon *Pg* infection. Understanding the effect of *Pg* infection on the regulation of osteoclast precursors will contribute to our understanding of *Pg*-induced bone loss and should help reveal novel diagnostic markers and therapeutic strategies to prevent bone loss associated with infection and inflammation.

## 2 | MATERIAL AND METHODS

### 2.1 | Mice

Wild-type (WT), MyD88 knockout (MyD88<sup>-/-</sup>), and OT-II transgenic mice, all on a C57BL/6 background, were bred and maintained within an environmentally controlled, pathogen-free animal facility at the University of Alabama at Birmingham (UAB). The original MyD88<sup>-/-</sup> breeding pairs were obtained under a material transfer agreement from

Dr Shikuo Akira (Osaka University, Osaka, Japan). Mice at 8-12 weeks of age were used in the studies. All studies were done according to the guidelines of the National Institutes of Health. Protocols were approved by the UAB Institutional Animal Care and Use Committee.

## 2.2 | Bacteria

*Pg* ATCC 33277 (from frozen stocks) was cultured and maintained on enriched trypticase soy agar plates (trypticase soy agar, 1% yeast extract, 5% defibrinated sheep blood, 5 µg/mL hemin, and 1 µg/mL menadione) at 37°C in an anaerobic atmosphere of 10% H<sub>2</sub>, 5% CO<sub>2</sub>, and 85% N<sub>2</sub>. For in vivo and in vitro studies, *Pg* was grown in trypticase soy broth (BD Biosciences) containing 1% yeast extract, 5 µg/mL hemin, and 2.5 µg/mL menadione. The bacteria were then harvested by centrifugation and washed with sterile phosphate-buffered saline (PBS). The number of bacteria (colony-forming units/mL) was determined by measuring the optical density (A) at 600 nm and extrapolating using a standard curve.

## 2.3 | Calvarial infection model

To induce bone loss, live *Pg* ( $1 \times 10^8$  CFU in 20 µL of PBS) was injected (using a Hamilton syringe) once daily for 6 days into the subcutaneous (s.c.) tissue over the left and right sides of the parietal bone (each side 10 µL) of anesthetized mice under isoflurane inhalation. Control mice were injected with vehicle (PBS). At different time points after the first injection of *Pg*, blood was collected from the tail veins. The interval of blood collections from each mouse was no <48 hours, and the frequency of blood collections from each mouse was no more than two time points. Serum was collected following centrifugation and stored at -20°C until assessed for cytokine levels. Mice were sacrificed for different analyses on day 3 following 2 days of *Pg* infection or on day 7 following 6 days of *Pg* infection.

## 2.4 | Histological assays

Mice were sacrificed on day 7, and the calvaria and adjacent connective tissues were dissected for histological assessment of inflammation and osteoclastogenic activity. Specifically, the tissues were fixed in 4% phosphate-buffered formalin and then decalcified in 10% EDTA. The parietal bones were bisected into rostral and caudal sides and embedded in paraffin. Five nonconsecutive coronal sections of 5 µm thickness were prepared. Sections were stained with hematoxylin and eosin (HE) or with a leukocyte acid phosphatase kit (Sigma-Aldrich) for tartrate-resistant acid phosphatase (TRAP) activity. TRAP-positive multinucleated cells (MNC,  $\geq 3$  nuclei) were counted as mature osteoclast. Images were acquired using a Nikon Eclipse 90i system (Nikon). Quantification of osteoclasts was performed on five randomly selected coronal sections/mouse and expressed as mean cell numbers per section.

TRAP staining of the whole calvarial bone without soft tissues was also done to assess the overall osteoclastogenic activity on calvaria after *Pg* infection.

## 2.5 | Micro-computed tomography (micro-CT) analysis

To evaluate *Pg*-induced bone loss, calvarial bone without soft tissues was fixed and then scanned using the Scanco µCT40 desktop cone-beam micro-CT scanner (Scanco Medical AG) using µCT Tomography v5.44. The scanning was carried out at 30-µm resolution, 70 kVp, and 114 µA with an integration time of 200 ms. Two hundred and ten slices were imaged. Scans were automatically reconstructed into 2D slices, and all slices were analyzed using the µCT Evaluation Program (v.6.5-2; Scanco Medical). The parameters measured were bone volume/total volume (BV/TV), area bone loss (mm<sup>2</sup>), and sagittal suture area (mm<sup>2</sup>).

## 2.6 | In vitro osteoclastogenesis assays

Mice were sacrificed on day 3 or day 7. Bone marrow and spleens from age-matched WT or MyD88<sup>-/-</sup> mice were harvested and processed as previously described.<sup>16,19</sup> Single-cell suspensions were prepared by mechanically dispersing the bone marrow or spleen through a 100-µm cell strainer. Red blood cells were lysed using flow cytometry mouse lysis buffer (R&D Systems). To induce osteoclast differentiation, cells were plated in 24-well plates at a density of  $2 \times 10^5$  cells/well for spleen cells or  $5 \times 10^4$  cells/well for bone marrow cells in  $\alpha$ -10 medium ( $\alpha$ -MEM, 10% FCS, 1 $\times$  PenStrep) supplemented with RANKL (100 ng/mL) and 10% culture supernatant from CMF14-12 cells as the source of M-CSF. Cells were cultured for 5-7 days and then stained for TRAP activity. TRAP<sup>+</sup> MNC were counted as mature osteoclasts. All experiment was done in triplicate.

To evaluate the function of osteoclasts, F-actin ring staining and the in vitro bone resorption assay were investigated. For F-actin ring staining, osteoclast differentiation was induced as described above for 6-8 days, and then fixed with 4% formaldehyde and permeabilized with 0.2% Triton X-100. Cells were then incubated with 2 U/mL rhodamine-phalloidin (Molecular Probes) at room temperature for 20 minutes. Actin ring staining was observed under a fluorescence microscope with the Leica Texas Red filter (Nikon Eclipse TE2000-E). For the in vitro bone resorption assay, cells were seeded on bovine cortical bone slices plated in 24-well culture plates, and osteoclast differentiation was induced as described above. Bone slices were harvested after 8-10 days in culture, and cells on bone slices were removed by sonication in PBS. Bone slices were then soaked in 0.3% H<sub>2</sub>O<sub>2</sub> for 30 minutes. Bone resorption pits were visualized by staining with 2 µg/mL peroxidase-conjugated wheat germ agglutinin (WGA) lectin (Sigma-Aldrich) for 1 hour and then developed with a DAB Peroxidase (HRP) Substrate Kit (Vector Laboratories). The percentage of bone

resorbed area on bone slices was determined using ImageJ analysis software (NIH).

## 2.7 | FACS analysis and cell sorting

Bone marrow and spleen cells were isolated from *Pg*-infected mice and control mice as described above, suspended in fluorescence-activated cell sorting (FACS) buffer, and stained with fluorescent-labeled antibodies against CD11b (clone M1/70), CD115 (c-fms; clone AFS98), CD265 (RANK; clone R12-31), Ly6C (clone HK1.4), and Ly6G (clone RB6-8C5). All FACS antibodies were purchased from eBioscience. Data were acquired using a BD LSR II flow cytometry (BD Bioscience) and analyzed using FlowJo software v10 (TreeStar). For cell sorting, BM or spleen cell suspensions from 3 mice/group were pooled together and then sorted for CD11b<sup>+</sup>c-fms<sup>+</sup>, CD11b<sup>+</sup>c-fms<sup>+</sup>RANK<sup>+</sup>, and CD11b<sup>+</sup>c-fms<sup>+</sup>RANK<sup>-</sup> cells using a FACS Aria IIIu cell sorter (BD Bioscience).

## 2.8 | CD4<sup>+</sup> T-cell proliferation assay

To evaluate the effect of osteoclast precursors on CD4<sup>+</sup> T-cell proliferation, single spleen cell suspensions from OT-II transgenic mice were cultured in RPMI 1640 medium at a concentration of  $2 \times 10^5$  cells/well in the presence or absence of the sorted CD11b<sup>+</sup>c-fms<sup>+</sup> cells from control and *Pg*-infected WT mice at a 1:1 ratio. OT-II transgenic mice have CD4<sup>+</sup> T cells with a T-cell receptor specific for the ovalbumin (OVA) sequence between residues 323-339.<sup>20</sup> The co-cultures were stimulated with the OVA<sub>323-339</sub> peptide (2.5 µg/mL) for 72 hours. CD4<sup>+</sup> T-cell proliferation was analyzed by measuring BrdU incorporation using a FITC BrdU staining kit for flow cytometry following the manufacturer's instructions (Invitrogen). Briefly, 10 µM BrdU was added to the cell cultures 24 hours prior to cell harvesting. Cells were then surface-stained with anti-mouse CD4 PerCP (BD Pharmingen), fixed, and permeabilized. After incubated with DNase I for 1 hours at 37°C, cells were intracellularly stained with anti-BrdU FITC. Data were acquired using a BD LSR II flow cytometry, and BrdU incorporation on CD4<sup>+</sup> T cells was analyzed using FlowJo software v10.

## 2.9 | Real-time PCR

To determine the induction of inflammatory genes following *Pg* infection, calvarial bone with periosteum from infected and noninfected mice was homogenized in TRIzol reagent (Invitrogen). Total RNA was extracted using RNeasy Mini Kit (Qiagen) according to the recommended procedure. cDNA was synthesized from 1 µg of total RNA by using the High Capacity cDNA Reverse Transcription Kits (Applied Biosystems). Real-time PCR was performed using a Lightcycler (Roche) with a FastStart DNA Master SYBR Green I reagent (Roche) for the expression of inflammatory and osteoclastogenic genes

including IL-1β, IL-6, TNF-α, and RANKL. Relative quantities of the tested genes were normalized to hypoxanthine-guanine phosphoribosyltransferase (HPRT) mRNA. The normalized data are expressed using the comparative  $2^{-\Delta\Delta CT}$  method. RANKL-induced expression of c-fms, RANK, and osteoclast genes including TRAP, MMP9, Ctsk, and Car2 in the cultures of osteoclast precursors was also analyzed using the same method described above.

## 2.10 | Cytokine analysis

To assess *Pg*-induced systemic inflammatory response, serum samples from infected and noninfected mice were collected and assessed for the levels of IL-1β, IL-6, IL-10, IL-12p40, TNF-α, and RANKL by ELISA, according to the manufacturer's instructions. Mouse IL-6, IL-10, IL-12p40, and TNF-α ELISA kits were purchased from eBioscience. Mouse IL-1β and RANKL Quantikine ELISA Kit was purchased from R&D Systems.

To determine *Pg*-induced cytokine response by osteoclast precursors, cells were plated at  $2 \times 10^5$  cell/well in 96-well plates and stimulated with the bacteria at an MOI of 50. Culture supernatants were collected after 24 hours and assessed for the levels of IL-6 and TNF-α.

## 2.11 | Statistical analysis

All results are reported as the mean ± SEM. Statistical significance was evaluated by ANOVA and the Tukey multiple-comparisons test using GraphPad Prism 6.02. *P*-values <.05 were considered significant.

# 3 | RESULTS

## 3.1 | Calvarial *Pg* infection results in localized inflammatory infiltration and osteoclastogenesis

Calvarial infection of mice with periodontal pathogens is a well-documented model to study host-microbial interactions.<sup>21</sup> In this study, we used this model to understand the mechanism of *Pg*-induced osteoclastogenesis. As shown in Figure 1A, a notable inflammatory infiltration of cells was observed in the soft tissues overlying the calvaria on day 7 following *Pg* infection of WT mice. A significant increase in the number of TRAP<sup>+</sup> multinuclear osteoclast formation was also noticed in the coronal calvarial sections following *Pg* infection (Figure 1B,C). In addition, areas of TRAP<sup>+</sup> multinuclear osteoclasts were observed in the whole-mount calvarial bone preparations following *Pg* infection (Figure 1D). Micro-CT analysis of calvarial bone showed areas of calvarial bone loss in *Pg*-infected mice, but not in control mice (Figure 1E). Significant differences were observed in calvarial bone volume/tissue volume (BV/TV), area of bone loss, and sagittal suture area, between *Pg*-infected mice and control mice (Figure 1F). Moreover, analysis of

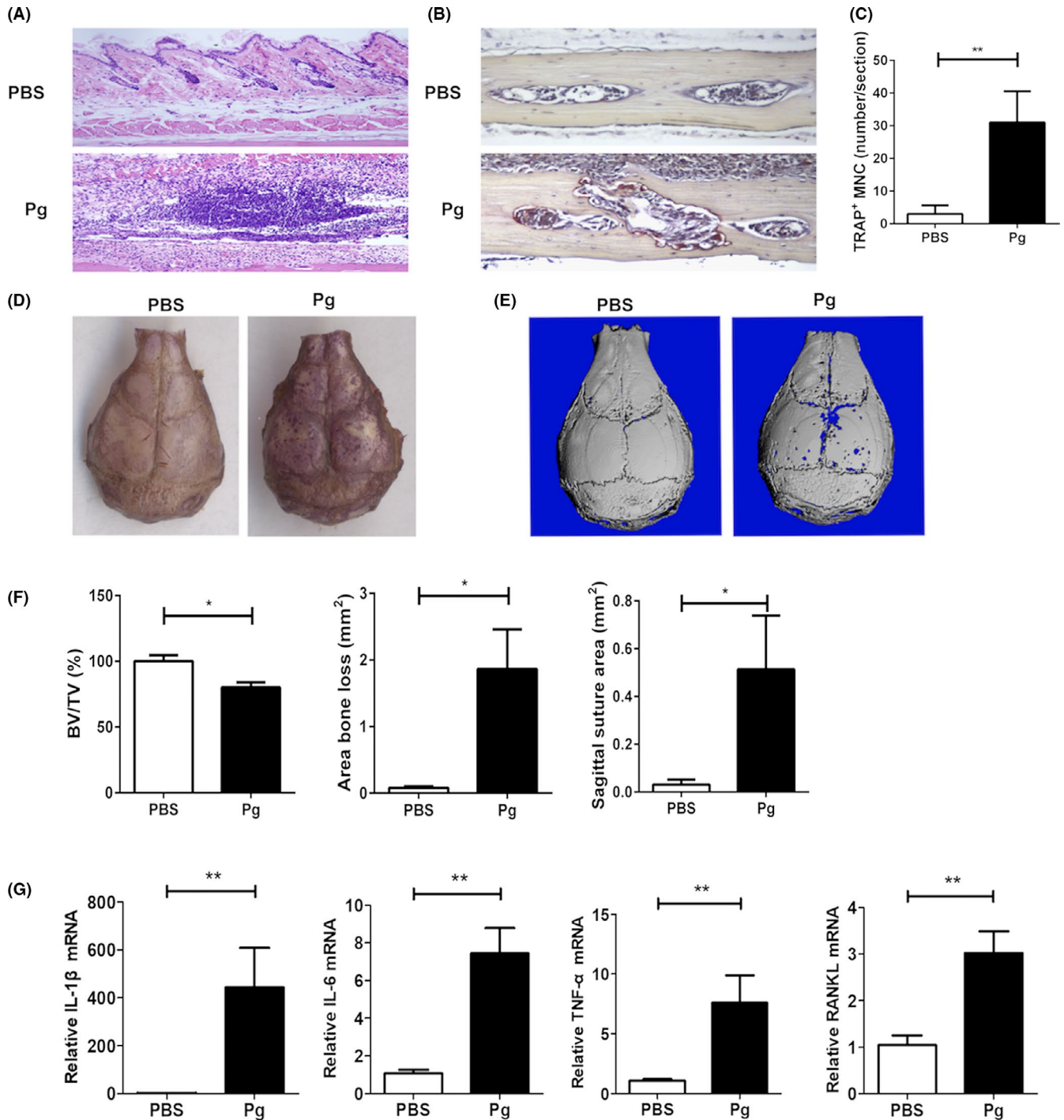


**FIGURE 1** Calvarial *Pg* infection results in localized inflammation and osteoclastogenesis. *Pg* ( $1 \times 10^8$  CFU in 20  $\mu$ L of PBS) was injected into the subcutaneous tissue over the left and right sides of the parietal bone of C57BL/6 WT mice once daily for 6 d. On day 7, parietal bone with or without the adjacent soft tissue was collected for histological analysis, RNA extraction, and micro-CT analysis. A, Representative images of coronal sections of HE staining. B, Representative TRAP staining of coronal sections. C, Quantification of TRAP-positive multinucleated cells (TRAP<sup>+</sup> MNC) on coronal sections. D, Representative images of whole calvaria TRAP activity. E, Representative micro-CT images of calvarial bone. F, Quantification of calvarial bone loss by bone volume/tissue volume (BV/TV), area bone loss, and sagittal suture area. G, The expression of IL-1 $\beta$ , IL-6, TNF- $\alpha$ , and RANKL mRNA in calvarial tissues. Data are expressed as the means  $\pm$  SEM ( $n \geq 6$ ). \*,  $P < .05$ ; \*\*,  $P < .01$

mRNA expression in calvarial tissues revealed that *Pg* infection induced significantly higher levels of inflammatory cytokine IL-1 $\beta$ , IL-6, TNF- $\alpha$ , and RANKL mRNA expression compared to the control group

(Figure 1G). These results demonstrate that induction of calvarial bone loss following *Pg* infection is associated with increased inflammation and osteoclast formation.

### 3.2 | Calvarial *Pg* infection increases the osteoclastogenic potential of bone marrow cells and splenocytes

Osteoclasts are multinucleated cells derived from myeloid precursors that are generated in bone marrow and travel to peripheral tissues through the bloodstream.<sup>22</sup> To understand the effect of calvarial *Pg* infection on the regulation of osteoclast precursors, we first performed *in vitro* osteoclastogenesis assays to compare the osteoclastogenic potential of bone marrow and spleen cells from *Pg*-infected and control WT mice. Bone marrow cells isolated from *Pg*-infected mice on day 3 showed a significantly increased number of TRAP<sup>+</sup> multinuclear osteoclast formation compared to cells from control mice (Figure 2A). A significant difference in osteoclast formation was observed on day 7 between bone marrow cells isolated from *Pg*-infected and control mice. In addition, a significant difference in osteoclast formation was noted between cells isolated on day 3 and day 7 from the bone marrow of *Pg*-infected mice. No significant difference in osteoclast formation was observed on day 3 in spleen cell cultures from infected and control mice (Figure 2B). However, splenocytes isolated on day 7 from *Pg*-infected mice showed significantly increased numbers of osteoclast formation compared to those isolated on day 7 from control mice, and from cells isolated on day 3 from *Pg*-infected mice. These results indicate that calvarial *Pg* infection increases the osteoclastogenic potential of bone marrow cells and peripheral splenic cells.

### 3.3 | Calvarial *Pg* infection increases the percentage and osteoclastogenic potential of CD11b<sup>+</sup>c-fms<sup>+</sup> cells from bone marrow and spleen

An increase in the osteoclastogenic potential of cells obtained from the bone marrow and spleens of *Pg*-infected mice could result from an increased percentage of osteoclast precursors, or from increased sensitivity of osteoclast precursors to osteoclast differentiation factors, or both. Osteoclast precursors are derived from multipotent hematopoietic stem cells in bone marrow through a series of differentiation stages including the differentiation of common myeloid progenitors and granulocyte/macrophage progenitors.<sup>4,5</sup> These stages have been characterized by changes in the surface expression of distinct markers. CD11b is a prominent marker for myeloid cells toward osteoclast lineage.<sup>23</sup> In addition, the conversion of c-fms<sup>-</sup> cells to c-fms<sup>+</sup> cells is an important landmark for osteoclast differentiation.<sup>22,23</sup> Therefore, we wanted to determine whether *Pg* infection regulates the percentage of CD11b<sup>+</sup>c-fms<sup>+</sup> cells in bone marrow and spleens. A significant increase in the percentage of CD11b<sup>+</sup> cells in bone marrow was observed after *Pg* infection on day 7 (Figure 3A). No significant difference was observed in the percentage of CD11b<sup>+</sup> cells in spleens of the control and the infected mice on either day 3 or day 7 (Figure 3B). Importantly, *Pg* infection induced a significant increase in the percentage of CD11b<sup>+</sup>c-fms<sup>+</sup> cells in the bone marrow on days 3 and 7 compared to controls (Figure 3A). In addition,

a significant increase in the percentage of CD11b<sup>+</sup>c-fms<sup>+</sup> cells was also seen in the spleen cells of *Pg*-infected mice on day 7 (Figure 3B). These results demonstrate that calvarial *Pg* infection induces the expansion of CD11b<sup>+</sup>c-fms<sup>+</sup> cells in bone marrow and spleen.

We next wanted to determine the osteoclastogenic potential of CD11b<sup>+</sup>c-fms<sup>+</sup> cells from control and *Pg*-infected WT mice. A significantly higher number of TRAP<sup>+</sup> multinuclear cells (MNC) were observed in cultures of CD11b<sup>+</sup>c-fms<sup>+</sup> cells derived from bone marrow of *Pg*-infected mice compared to those of noninfected controls (Figure 4A). To evaluate the function of these osteoclasts, F-actin ring staining and an *in vitro* bone resorption assay were done. Actin ring formation is a prerequisite for osteoclast bone resorption.<sup>24</sup> A significantly increased number of osteoclasts with actin ring formation were seen in cultures of CD11b<sup>+</sup>c-fms<sup>+</sup> cells from the bone marrow of *Pg*-infected mice compared to cultures of noninfected control mice (Figure 4B). Moreover, the *in vitro* bone resorption assay showed that the total bone resorption area on bone slices in the culture of CD11b<sup>+</sup>c-fms<sup>+</sup> cells from *Pg*-infected mice was significantly higher than that from the control group (Figure 4C). Similar results were seen with CD11b<sup>+</sup>c-fms<sup>+</sup> cells sorted from spleens (data not shown). Collectively, these results indicate that *Pg* infection not only induces an expansion of CD11b<sup>+</sup>c-fms<sup>+</sup> cells in bone marrow and spleen, but also increases the osteoclastogenic potential of these cells.

### 3.4 | CD11b<sup>+</sup>c-fms<sup>+</sup>RANK<sup>+</sup> and CD11b<sup>+</sup>c-fms<sup>+</sup>RANK<sup>-</sup> cells have similar osteoclastogenic potential

It has been suggested that multiple populations of osteoclast precursors with different osteoclastogenic potential are present within the murine bone marrow and that there is a possible developmental relationship between the different populations, characterized by changes in the surface expression of distinct markers.<sup>25</sup> In addition to the expression of M-CSF receptor c-fms, RANK is considered as another critical landmark during osteoclast differentiation. RANK is a member of the TNF-receptor superfamily of proteins and the only known receptor for RANKL.<sup>26</sup> M-CSF is a potent stimulator of RANK expression in osteoclast precursors, and then ligation of RANKL to RANK on the surface of osteoclast precursors results in the activation of multiple signaling cascades and transcription factors including NF- $\kappa$ B and NFATc1, which are essential for osteoclast formation. Recent studies have suggested that the cell surface expression of RANK is a key feature of lineage-committed osteoclast precursors.<sup>27,28</sup> Unlike the c-fms<sup>+</sup>RANK<sup>-</sup> cells, which are identified as osteoclast precursors at an earlier stage, c-fms<sup>+</sup>RANK<sup>+</sup> cells are thought to be at a more advanced stage of osteoclast development that can promptly differentiate into osteoclasts in response to bone resorption stimuli *in vivo*.<sup>27,28</sup> Thus, we next sought to determine whether *Pg* infection induces the expansion of CD11b<sup>+</sup>c-fms<sup>+</sup>RANK<sup>+</sup> cell population. Our results show that *Pg* infection significantly increased the percentage of CD11b<sup>+</sup>c-fms<sup>+</sup>RANK<sup>-</sup> cells in the bone marrow on days 3 and 7 (Figure 5A). Similar results were seen with

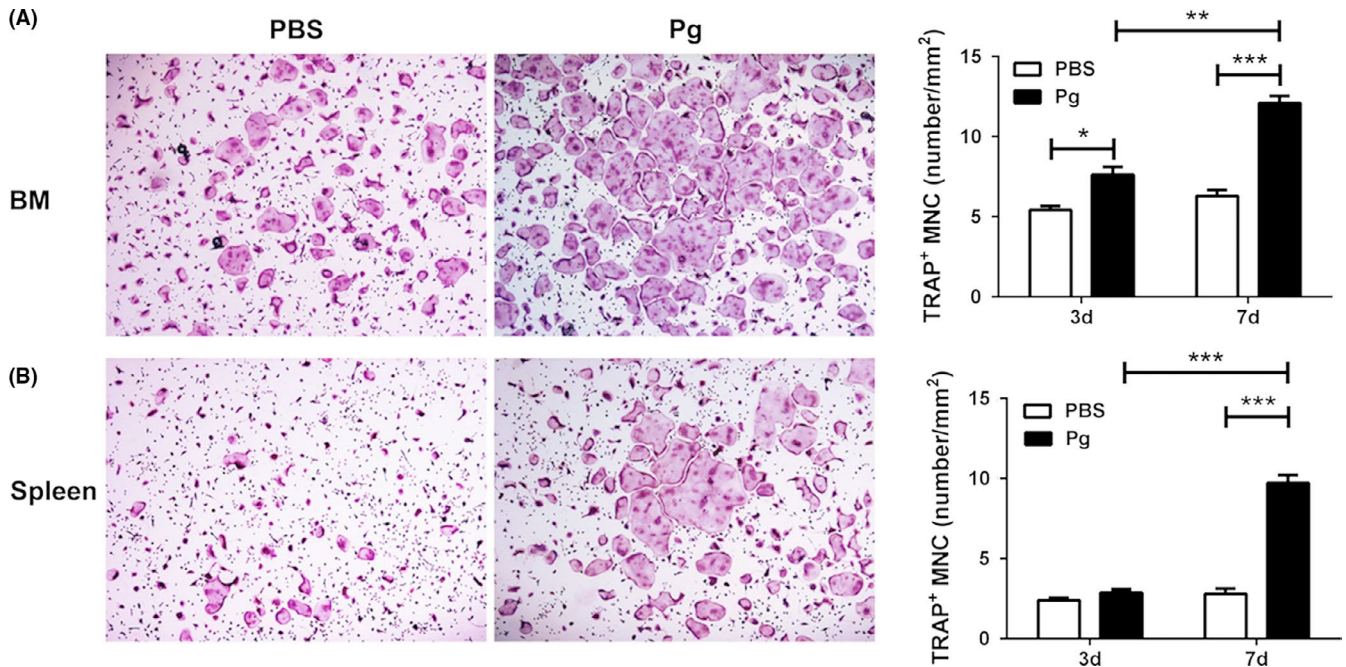


**FIGURE 2** Calvarial *Pg* infection of WT mice increases the osteoclastogenic potential of bone marrow (BM) and spleen cells. BM and spleen cells were harvested on days 3 and 7 from *Pg*-infected and noninfected mice. Cells were cultured with M-CSF and RANKL and stained for TRAP activity on day 5 (BM cells) or on day 7 (spleen cells). A, TRAP<sup>+</sup> MNC in BM cell cultures. B, TRAP<sup>+</sup> MNC in spleen cell cultures. A representative area of cultures of BM (A) and spleen (B) cells harvested on day 7 of infection at 40x magnification is shown. Data are expressed as the means  $\pm$  SEM ( $n \geq 6$ ). \*,  $P < .05$ ; \*\*,  $P < .01$ ; \*\*\*,  $P < .001$

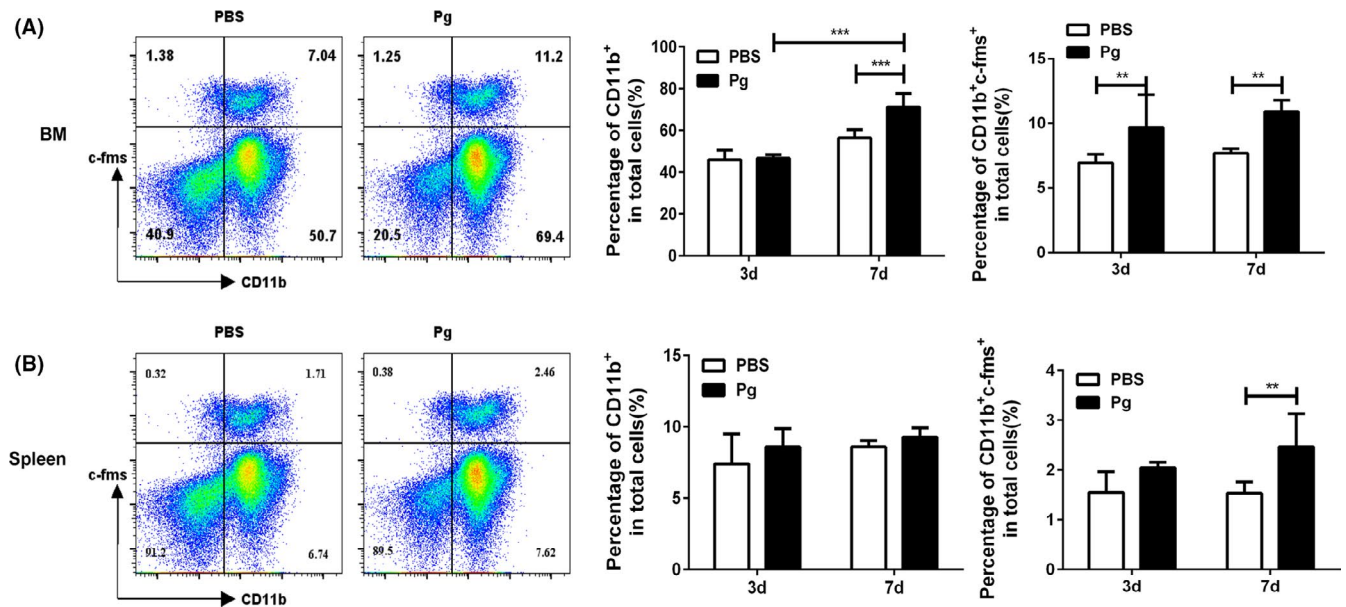


**FIGURE 3** Calvarial *Pg* infection of WT mice induces the expansion of CD11b<sup>+</sup>c-fms<sup>+</sup> cells in BM and spleen. BM and spleen cells were harvested on days 3 and 7 from *Pg*-infected and noninfected mice. A, The percentage of CD11b<sup>+</sup> cells and CD11b<sup>+</sup>c-fms<sup>+</sup> cells in BM. B, The percentage of CD11b<sup>+</sup> cells and CD11b<sup>+</sup>c-fms<sup>+</sup> cells in spleen. Data are expressed as the means  $\pm$  SEM ( $n \geq 6$ ). \*\*,  $P < .01$ ; \*\*\*,  $P < .001$

spleen cells on day 7 (Figure 5B). However, although the percentage of CD11b<sup>+</sup>c-fms<sup>+</sup>RANK<sup>+</sup> cells in the bone marrow (on days 3 and 7) and spleen cells (on day 7) was higher in *Pg*-infected mice than the control mice, no significant difference was attained.

We have previously demonstrated that noncommitted osteoclast precursors and lineage-committed osteoclast precursors have

distinct features in response to *Pg* stimulation.<sup>19</sup> In this regard, *Pg* inhibits noncommitted osteoclast precursors to differentiate into mature osteoclasts, but potentiates osteoclast differentiation of RANKL-committed osteoclast precursors. In addition, committed osteoclast precursors lose the ability to produce cytokines in response to *Pg*. To determine whether CD11b<sup>+</sup>c-fms<sup>+</sup>RANK<sup>+</sup> cells

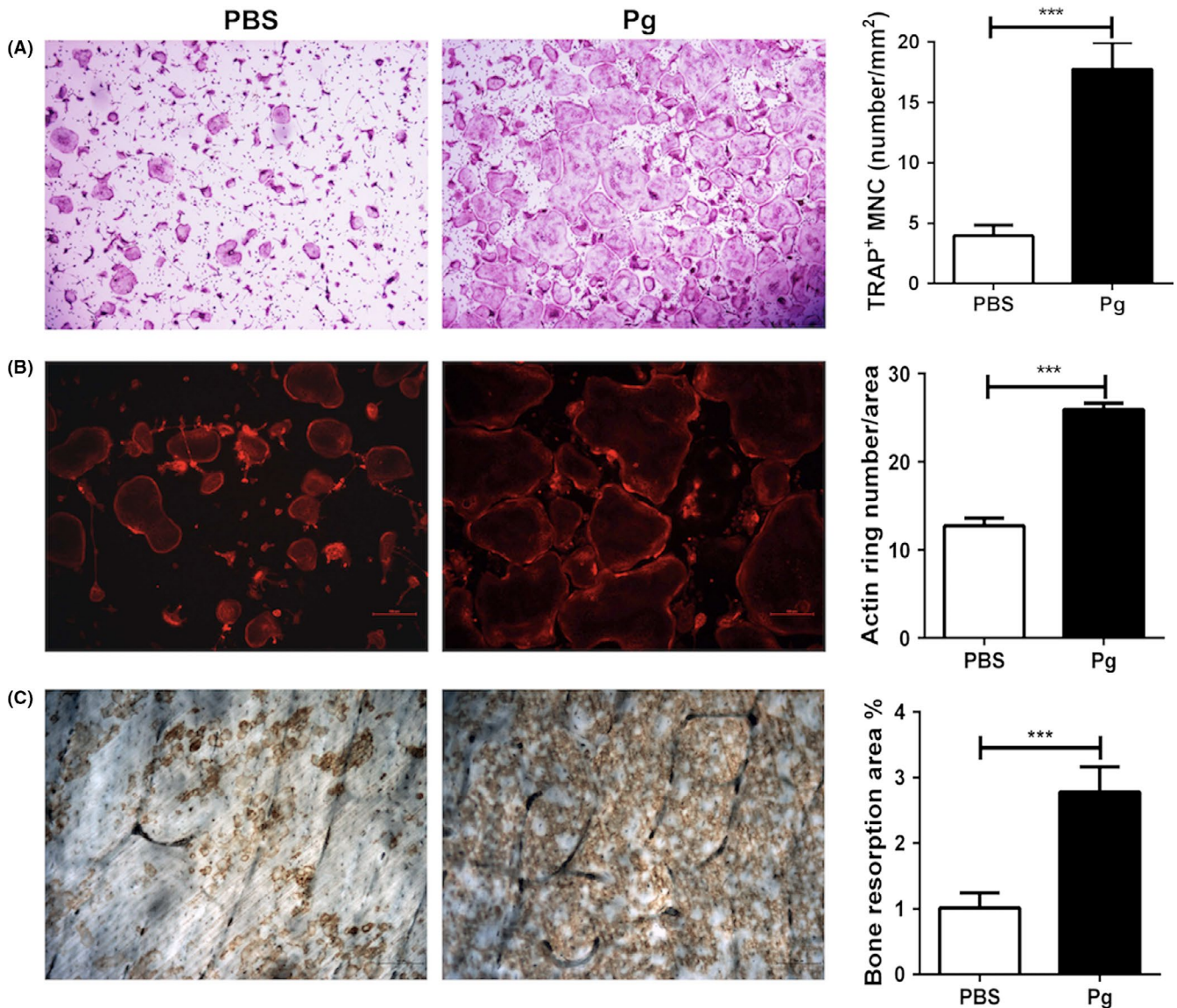
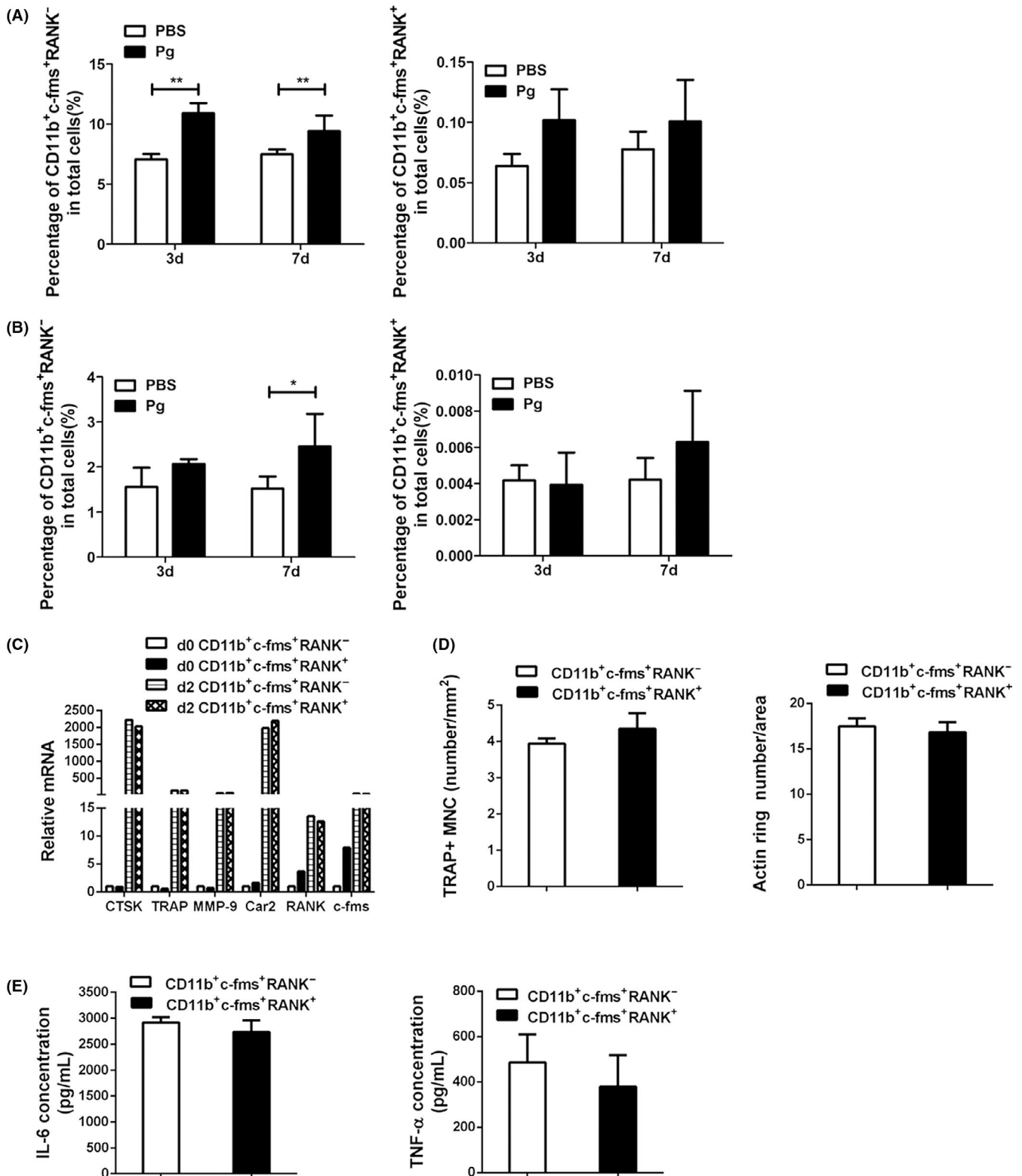


**FIGURE 4** Pg infection of WT mice enhances the osteoclastogenic potential of CD11b<sup>+</sup>c-fms<sup>+</sup> cells. BM cells were harvested on day 7 from Pg-infected and noninfected mice. Cells from 3 mice/group were pooled and sorted for CD11b<sup>+</sup>c-fms<sup>+</sup> cells. CD11b<sup>+</sup>c-fms<sup>+</sup> cells were then cultured in triplicate with M-CSF and RANKL in 24-well plate with or without bone slices for 5-7 d, and stained for TRAP activity, F-actin ring formation, or wheat germ agglutinin (WGA). A, Representative images and quantification of TRAP<sup>+</sup> MNC in the cell cultures without bone slices. B, Representative images and quantification of actin rings in the cell cultures without bone slices. C, Representative images and quantification of area of WGA staining on bone slices. Data are expressed as the means  $\pm$  SEM of three independent experiments. \*\*\*,  $P < .001$

**FIGURE 5** CD11b<sup>+</sup>c-fms<sup>+</sup>RANK<sup>-</sup> and CD11b<sup>+</sup>c-fms<sup>+</sup>RANK<sup>+</sup> cells have similar osteoclastogenic potential and ability to produce inflammatory cytokines. BM and spleen cells were harvested on days 3 and 7 from Pg-infected and noninfected WT mice, and analyzed for the expression of CD11b, c-fms, and RANK by FACS. Day 7 BM cell suspensions from 3 mice/group were pooled and sorted for CD11b<sup>+</sup>c-fms<sup>+</sup>RANK<sup>-</sup> and CD11b<sup>+</sup>c-fms<sup>+</sup>RANK<sup>+</sup> cells. Cells were then cultured in triplicate with RANKL to induce osteoclast differentiation, or with Pg to induce cytokine production. A, The percentage of CD11b<sup>+</sup>c-fms<sup>+</sup>RANK<sup>-</sup> and CD11b<sup>+</sup>c-fms<sup>+</sup>RANK<sup>+</sup> cells in BM. B, The percentage of CD11b<sup>+</sup>c-fms<sup>+</sup>RANK<sup>-</sup> and CD11b<sup>+</sup>c-fms<sup>+</sup>RANK<sup>+</sup> cells in spleen. C, The expression of osteoclast genes (Ctsk, TRAP, MMP9, and Car2), as well as c-fms and RANK by CD11b<sup>+</sup>c-fms<sup>+</sup>RANK<sup>-</sup> and CD11b<sup>+</sup>c-fms<sup>+</sup>RANK<sup>+</sup> cells at the baseline (d0) and after 48 h of RANKL stimulation (d2). D, Quantification of RANKL-induced osteoclast formation following TRAP staining and F-actin ring staining. E, The levels of IL-6 and TNF- $\alpha$  production in the culture supernatants of CD11b<sup>+</sup>c-fms<sup>+</sup>RANK<sup>-</sup> and CD11b<sup>+</sup>c-fms<sup>+</sup>RANK<sup>+</sup> cells following 24 h of Pg (MOI = 50) stimulation. Data in A and B are expressed as the means  $\pm$  SEM ( $n \geq 6$ ). Data in C are representative of three independent experiments. Data in D and E are expressed as the means  $\pm$  SEM of three independent experiments. \*,  $P < .05$ ; \*\*,  $P < .01$



are precursor cells that have committed to the osteoclast lineage, CD11b<sup>+</sup>c-fms<sup>+</sup>RANK<sup>+</sup> and CD11b<sup>+</sup>c-fms<sup>+</sup>RANK<sup>-</sup> cells were sorted out from bone marrow cells from WT mice and cultured with M-CSF and RANKL in the absence or presence of *Pg* to induce osteoclast differentiation. In addition, *Pg*-induced cytokine production by CD11b<sup>+</sup>c-fms<sup>+</sup>RANK<sup>+</sup> and CD11b<sup>+</sup>c-fms<sup>+</sup>RANK<sup>-</sup> cells was assessed. Our results showed that there was no significant difference in

RANKL-induced expression of osteoclast genes including *Ctsk*, *TRAP*, *MMP9*, and *Car2* by CD11b<sup>+</sup>c-fms<sup>+</sup>RANK<sup>+</sup> and CD11b<sup>+</sup>c-fms<sup>+</sup>RANK<sup>-</sup> cells (Figure 5C). Similar levels of *c-fms* and *RANK* mRNA expression were induced in CD11b<sup>+</sup>c-fms<sup>+</sup>RANK<sup>+</sup> and CD11b<sup>+</sup>c-fms<sup>+</sup>RANK<sup>-</sup> cells (Figure 5C). In addition, similar numbers of osteoclast formation were observed from CD11b<sup>+</sup>c-fms<sup>+</sup>RANK<sup>+</sup> and CD11b<sup>+</sup>c-fms<sup>+</sup>RANK<sup>-</sup> cells (Figure 5D). Furthermore, in the presence

of *Pg*, no osteoclast formation and osteoclast gene induction were induced by RANKL in both cell cultures (data not shown). Moreover, *Pg* stimulation induced similar levels of IL-6 and TNF- $\alpha$  in the cultures of CD11b<sup>+</sup>c-fms<sup>+</sup>RANK<sup>+</sup> and CD11b<sup>+</sup>c-fms<sup>+</sup>RANK<sup>-</sup> cells (Figure 5E). Taken together, these results suggest that CD11b<sup>+</sup>c-fms<sup>+</sup>RANK<sup>+</sup> and CD11b<sup>+</sup>c-fms<sup>+</sup>RANK<sup>-</sup> are osteoclast precursors with similar osteoclastogenic and pro-inflammatory potential.

### 3.5 | CD4<sup>+</sup> T-cell suppressive function of CD11b<sup>+</sup>c-fms<sup>+</sup> cells

Myeloid-derived suppressor cells (MDSC) are one of the dominant immunosuppressive cell populations that rapidly expand under infectious and inflammatory conditions, especially in chronic infections.<sup>29,30</sup> We have recently shown that 14 days of subcutaneous *Pg* infection induces the expansion of three subpopulations of MDSC (CD11b<sup>+</sup>Ly6C<sup>++</sup>Ly6G<sup>+</sup>, CD11b<sup>+</sup>Ly6C<sup>+</sup>Ly6G<sup>++</sup>, and CD11b<sup>+</sup>Ly6C<sup>+</sup>Ly6G<sup>+</sup>) in mouse bone marrow and spleen and that the CD11b<sup>+</sup>Ly6C<sup>++</sup>Ly6G<sup>+</sup> monocytic MDSC not only have T-cell suppressive function, but also have the plasticity to differentiate into osteoclasts.<sup>31</sup> Therefore, we next wanted to determine whether CD11b<sup>+</sup>c-fms<sup>+</sup> cells are a subpopulation of MDSC. Our results show that over 80% of CD11b<sup>+</sup>c-fms<sup>+</sup> cells are Ly6C<sup>++</sup>Ly6G<sup>+</sup>, whereas <1% of CD11b<sup>+</sup>c-fms<sup>+</sup> cells are Ly6C<sup>+</sup>Ly6G<sup>++</sup> (Figure 6A). Consistently, more than 80% of CD11b<sup>+</sup>Ly6C<sup>++</sup>Ly6G<sup>+</sup> cells were c-fms<sup>+</sup>, whereas <1% of CD11b<sup>+</sup>Ly6C<sup>+</sup>Ly6G<sup>++</sup> cells were c-fms<sup>-</sup> (Figure 6B). To assess whether CD11b<sup>+</sup>c-fms<sup>+</sup> cells have similar immunosuppressive function as CD11b<sup>+</sup>Ly6C<sup>++</sup>Ly6G<sup>+</sup> MDSC, we evaluated the effect of these cells on CD4<sup>+</sup> T-cell proliferation. Our results showed that stimulation of OT-II splenocytes with OVA<sub>323-339</sub> peptide significantly enhanced OT-II CD4<sup>+</sup> T-cell proliferation (Figure 6C). Co-culture of OT-II splenocytes with bone marrow-derived CD11b<sup>+</sup>c-fms<sup>+</sup> cells from noninfected WT mice significantly inhibited OVA-specific OT-II CD4<sup>+</sup> T-cell proliferation. In addition, co-culture of OT-II splenocytes with bone marrow-derived CD11b<sup>+</sup>c-fms<sup>+</sup> cells from *Pg*-infected mice showed a significantly greater inhibition of OVA-specific CD4<sup>+</sup> T-cell proliferation than that observed with CD11b<sup>+</sup>c-fms<sup>+</sup> cells from noninfected mice. Similar results were observed with splenic CD11b<sup>+</sup>c-fms<sup>+</sup> cells (data not shown). Our results indicate that the majority of CD11b<sup>+</sup>c-fms<sup>+</sup> cells are monocytic MDSC and that calvarial *Pg* infection potentiates the immunosuppressive ability of these cells on antigen-specific CD4<sup>+</sup> T-cell proliferation.

### 3.6 | Calvarial *Pg* infection induces minimal systemic inflammation and bone loss

It has been previously suggested that systemic TNF- $\alpha$  can induce an increased number of circulating CD11b<sup>high</sup> osteoclast precursors, which contribute to bone loss and erosion in inflammatory arthritis.<sup>22,23</sup> Therefore, we wondered whether calvarial *Pg* infection increased the levels of systemic TNF- $\alpha$ , thus leading to the expansion of osteoclast

precursors in bone marrow and spleen. We also wanted to determine whether calvarial *Pg* infection induces osteoclastogenic activity and bone loss in long bones. Our results show that daily *Pg* infection of WT mice induced a transient but significant increase in the level of serum IL-6, but this increase dropped down on day 7 (Figure 7A). Very low levels of TNF- $\alpha$ , IL-10, and IL-12p40 were detected in serum at all time points after *Pg* infection (data not shown). In addition, no difference was observed in the level of serum RANKL between infected and noninfected mice (Figure 7B). These data suggest that the expansion of CD11b<sup>+</sup>c-fms<sup>+</sup> population following calvarial *Pg* infection is unlikely due to the systemic induction of TNF- $\alpha$  or RANKL. Moreover, no significant difference in the TRAP<sup>+</sup> osteoclast formation and bone loss was observed in the cortical or trabecular bone area of long bones in *Pg*-infected mice as compared to control mice (Figure 7C-F). These results indicate that although calvarial *Pg* infection induces a systemic expansion of osteoclast precursors, significant bone loss occurs only at the local infection/inflammation sites, and not systemically, at least under the current experimental condition.

### 3.7 | MyD88 is involved in *Pg*-mediated regulation of osteoclast precursors and calvarial bone loss

Toll-like receptor (TLR) signaling is at the core of the interactions between bacterial pathogens and the host.<sup>32</sup> Activation of TLR triggers an innate immune response via different signaling components, such as the myeloid differentiation factor 88 (MyD88) and the Toll/IL-1R domain-containing adaptor-inducing IFN- $\beta$  (TRIF). The MyD88-dependent signaling pathway is utilized by all known TLRs except TLR3, while the TRIF-mediated pathway, which is commonly known as the MyD88-independent pathway, plays an essential role in TLR3- and TLR4-mediated downstream signaling. Although TLR2 and TLR4 are believed to be the major TLRs involved in the host immune response to *Pg*,<sup>33,34</sup> there is much controversy about the involvement of TLR2/TLR4 in host inflammatory responses and bone loss following *Pg* infection.<sup>35-38</sup> In addition, no study has looked at the role of TLR signaling in the regulation of osteoclast precursors following *Pg* infection in vivo. We have previously reported that TLR2/MyD88, but not TLR4/TRIF, is the central pathway involved in *Pg*-mediated regulation of osteoclast differentiation in vitro.<sup>19</sup> Here, we sought to investigate the role of MyD88 in the regulation of osteoclast precursors and osteoclastogenesis following *Pg* infection in vivo. Similar numbers of TRAP<sup>+</sup> multinuclear cells were seen in cultures of bone marrow (Figure 8A) and spleen (Figure 8B) cells from WT and MyD88<sup>-/-</sup> control mice in the presence of M-CSF and RANKL. However, calvarial *Pg* infection induced a significant increase in the osteoclastogenic potential of bone marrow and spleen cells from WT mice, but not from MyD88<sup>-/-</sup> mice. In addition, unlike WT-infected mice, no significant increase in the percentage of CD11b<sup>+</sup>c-fms<sup>+</sup> cells was observed in the bone marrow and spleen cells from MyD88<sup>-/-</sup> mice infected with *Pg* (Figure 8C,D). Furthermore, no significant increase in the gene expression of the inflammatory cytokines and

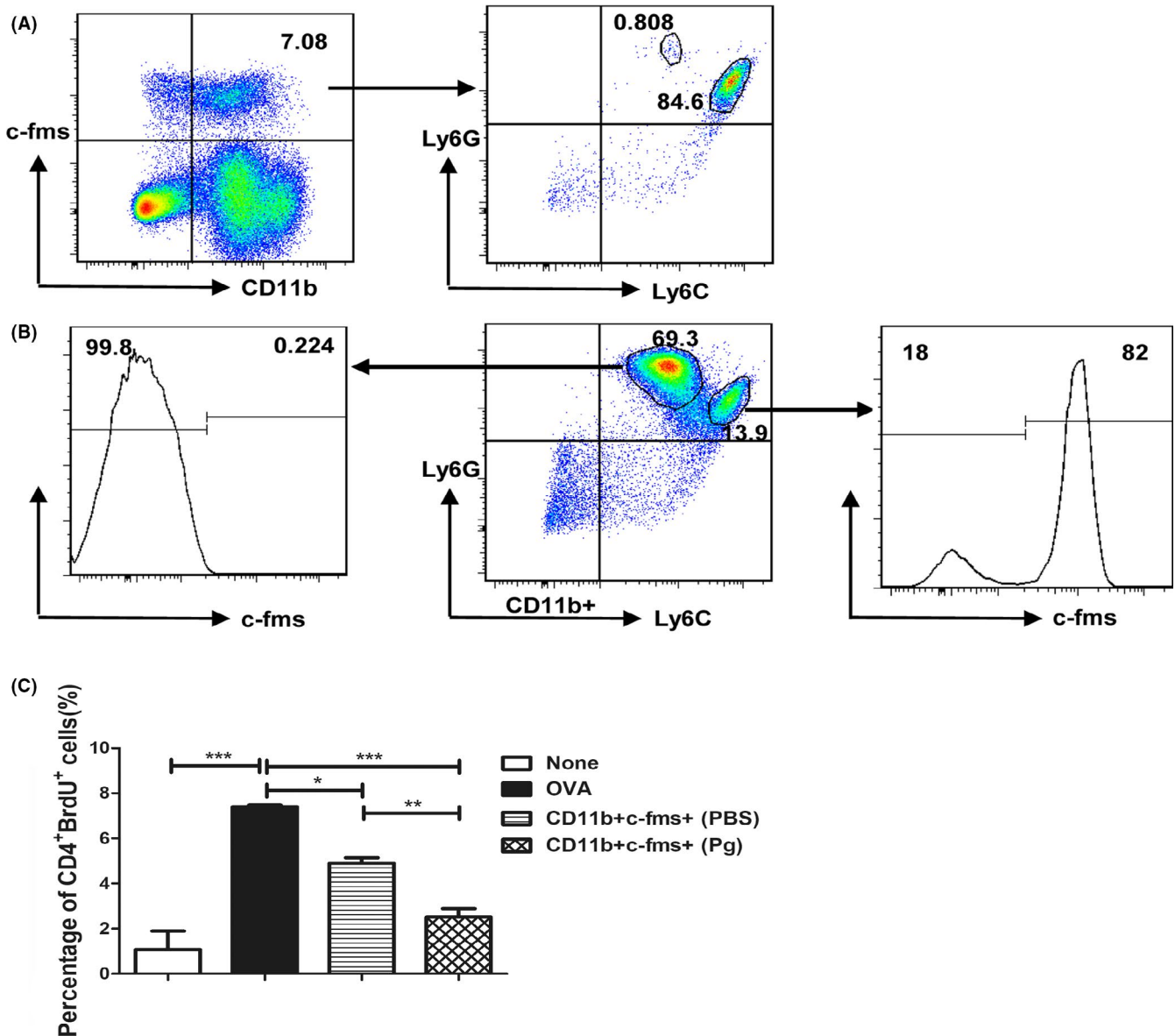


**FIGURE 6** CD11b<sup>+</sup>c-fms<sup>+</sup> osteoclast precursors are a subpopulation of MDSC. BM cells were harvested and analyzed for the expression of CD11b, c-fms, Ly6C, and Ly6G by FACS. CD11b<sup>+</sup>c-fms<sup>+</sup> cells were sorted from the BM of *Pg*-infected and noninfected WT mice on day 7 and co-cultured with spleen cells from OT-II mice. The cultures were stimulated with the OVA<sub>323-339</sub> peptide for 72 h, and BrdU was added during the last 24 h. Control cultures included OT-II spleen cells with or without the OVA<sub>323-339</sub> peptide. OVA-specific CD4<sup>+</sup> T-cell proliferation in the presence and absence of CD11b<sup>+</sup>c-fms<sup>+</sup> cells was analyzed by assessing the percentage of BrdU-incorporated CD4<sup>+</sup> T cells by FACS. A, Representative flow cytometric plots showing percentage of Ly6C<sup>++</sup>Ly6G<sup>+</sup> and Ly6C<sup>+</sup>Ly6G<sup>++</sup> cells in CD11b<sup>+</sup>c-fms<sup>+</sup> cells. B, Representative flow cytometric plots showing percentage of c-fms<sup>+</sup> cells in CD11b<sup>+</sup>Ly6C<sup>++</sup>Ly6G<sup>+</sup> and CD11b<sup>+</sup>Ly6C<sup>+</sup>Ly6G<sup>++</sup> cells. C, Percentage of BrdU incorporation in CD4<sup>+</sup> cells. Data are expressed as the means ± SEM from three independent experiments. \*,  $P < .05$ ; \*\*,  $P < .01$ ; \*\*\*,  $P < .001$

osteoclastogenic markers was observed in the calvarial tissues from MyD88<sup>-/-</sup> mice following *Pg* infection (Figure 8E). Moreover, contrary to the significant bone loss observed in the calvaria of WT-infected mice, no significant bone loss was detected in the calvarial bone of MyD88<sup>-/-</sup> mice following *Pg* infection (Figure 8F,G). Lastly, no induction of serum IL-6 was detected in MyD88<sup>-/-</sup> mice following *Pg* infection (data not shown). These results demonstrate that MyD88 is involved in *Pg*-mediated upregulation of osteoclast precursors and inflammation, as well as calvarial bone loss.

## 4 | DISCUSSION

Monocytes, macrophages, and DC are known to respond to pathogenic insult by expanding their effector populations and by secreting factors to eliminate infection.<sup>39</sup> However, beyond the knowledge that osteoclasts are differentiated from the monocyte/macrophage lineage of HSC and share common ancestry with macrophages and DC, the nature and function of osteoclast precursors are not completely understood. Furthermore, little is known about how

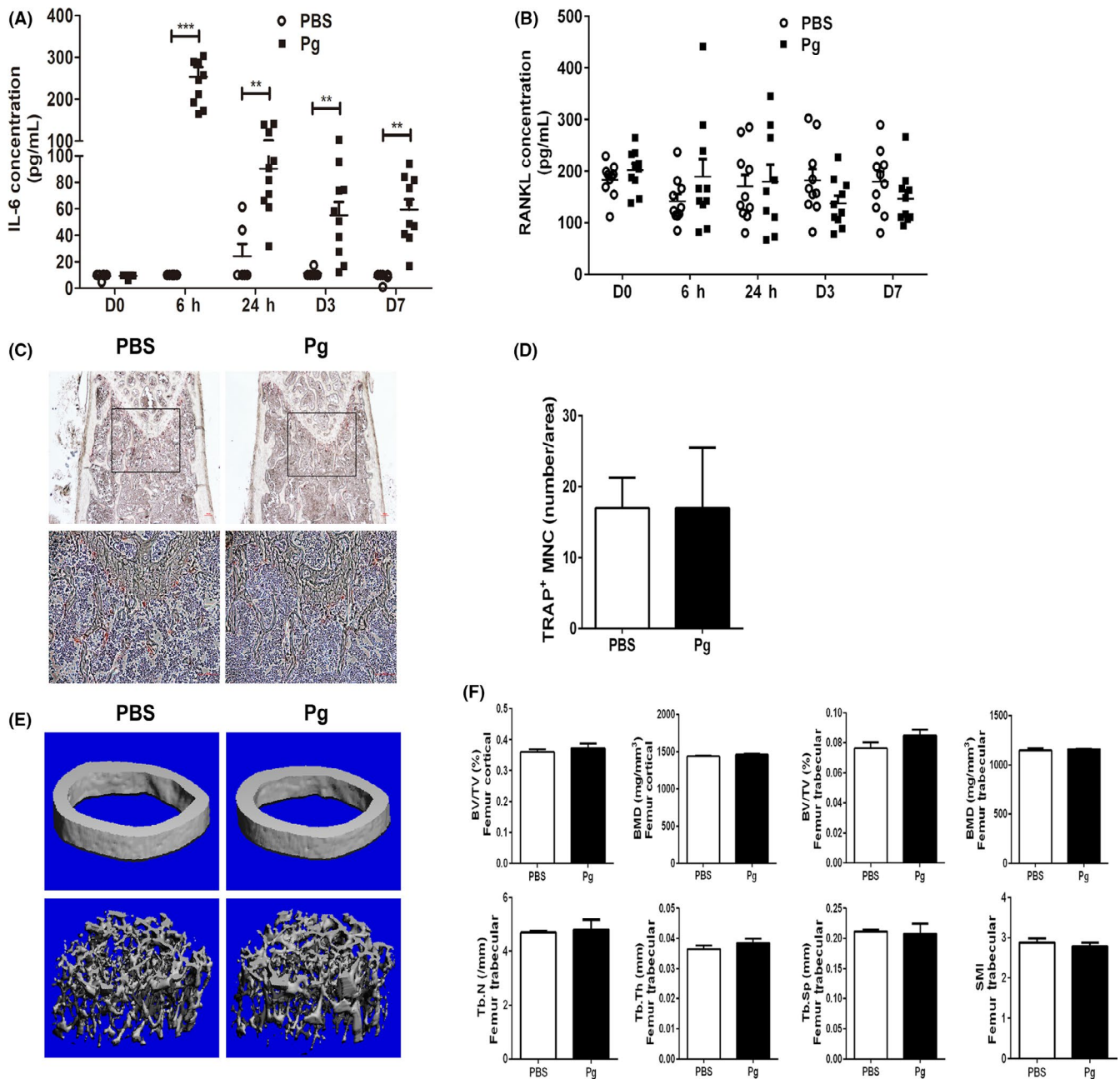


**FIGURE 7** Calvarial *Pg* infection induces minimal systemic inflammation and osteoclastogenesis. Serum samples were collected before, and at 6 h, 24 h, and on day 3 and day 7 after *Pg* infection of WT mice. Serum IL-6 and RANKL levels were analyzed by ELISA. Femurs were isolated for histological and micro-CT analysis. A, Serum IL-6 levels. \*\*,  $P < .01$ ; \*\*\*,  $P < .001$ . B, Serum RANKL levels. C, Representative TRAP staining of femur sections. D, Quantification of TRAP<sup>+</sup> MNC/area as shown in C. E, Representative micro-CT analysis of femurs. F, Quantification of bone loss in femurs. BV/TV, bone volume/tissue volume; BMD, bone mineral density; Tb.N, trabecular number; Tb.Th, trabecular thickness; Tb.Sp, trabecular separation; SMI, structure model index. Data in D and F are expressed as the means  $\pm$  SEM ( $n = 4$ )

osteoclast precursors respond to bacterial infection *in vivo*. In the present study, we demonstrated that calvarial *Pg* infection of mice increased the number and osteoclastogenic potential of CD11b<sup>+</sup>c-fms<sup>+</sup> osteoclast precursors in bone marrow and spleen, suggesting that the increased frequency and function of osteoclast precursors contribute to the pathogenesis of *Pg* infection-mediated bone loss.

It has been shown previously that human peripheral blood mononuclear cells expressing relatively high levels of RANK develop more and larger osteoclasts than cells expressing moderate to low levels

of RANK in response to exogenous RANKL, indicating that RANK-expressing cells are predisposed to osteoclast differentiation.<sup>40</sup> In addition, Mizoguchi et al<sup>28</sup> showed that bone marrow cells that are double-positive for c-fms and RANK are cell cycle-arrested quiescent lineage-committed osteoclast precursors. However, our results showed that CD11b<sup>+</sup>c-fms<sup>+</sup>RANK<sup>+</sup> and CD11b<sup>+</sup>c-fms<sup>+</sup>RANK<sup>-</sup> have similar osteoclastogenic potential. This finding is in agreement with that reported by Muto et al,<sup>27</sup> showing that bone marrow RANK<sup>high</sup>c-fms<sup>low</sup> cells have similar osteoclastogenic potential as RANK<sup>low</sup>c-fms<sup>high</sup>

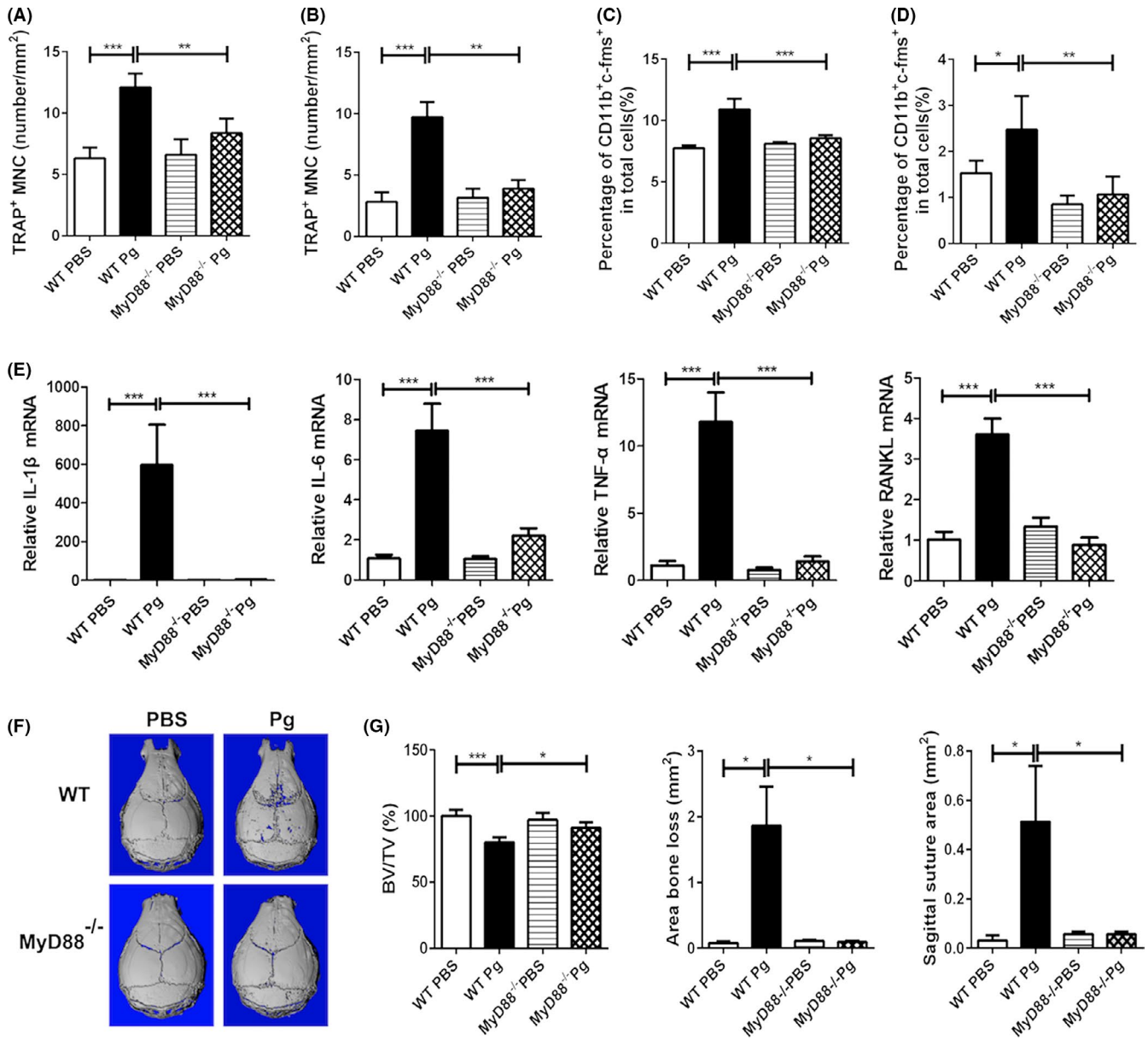


**FIGURE 8** MyD88 is involved in *Pg*-induced expansion of CD11b<sup>+</sup>c-fms<sup>+</sup> cells and calvarial bone loss. BM and spleen cells, and parietal bone and the adjacent soft tissue from *Pg*-infected and noninfected WT and MyD88<sup>-/-</sup> mice were harvested on day 7. A, Quantification of RANKL-induced TRAP<sup>+</sup> MNC formation from BM cells. B, Quantification of RANKL-induced TRAP<sup>+</sup> MNC formation from splenocytes. C, Percentage of CD11b<sup>+</sup>c-fms<sup>+</sup> cells in BM. D, Percentage of CD11b<sup>+</sup>c-fms<sup>+</sup> cells in spleen. E, Quantification of the expression of IL-1 $\beta$ , IL-6, TNF- $\alpha$ , and RANKL mRNA in calvarial tissues. F, Representative of micro-CT analysis of calvarial bone. G, Quantification of calvarial bone loss by BV/TV, area bone loss, and sagittal suture area. Data are expressed as the means  $\pm$  SEM ( $n = 6$ ). \*,  $P < .05$ ; \*\*,  $P < .01$ ; \*\*\*,  $P < .001$

cells. Our results further showed that CD11b<sup>+</sup>c-fms<sup>+</sup>RANK<sup>+</sup> and CD11b<sup>+</sup>c-fms<sup>+</sup>RANK<sup>-</sup> have a similar ability to produce pro-inflammatory cytokines in response to *Pg* stimulation. Since lineage-determined osteoclast precursors lose their ability to produce inflammatory cytokines,<sup>19</sup> it therefore seems implausible that CD11b<sup>+</sup>c-fms<sup>+</sup>RANK<sup>+</sup> cells are lineage-determined osteoclast precursors. Based on our studies and the literature,<sup>19,26,41</sup> it is likely that ligation of RANKL to RANK followed by inducing the expression of osteoclast genes is indispensable for the lineage determination of osteoclast precursors.

Previous studies have shown that serum TNF- $\alpha$  can increase the number of circulating CD11b<sup>+</sup> osteoclast precursors in inflammatory

arthritis.<sup>22,23</sup> However, in the present study, serum TNF- $\alpha$  was not detected following calvarial *Pg* infection, suggesting that the expansion of CD11b<sup>+</sup>c-fms<sup>+</sup> cells in the current model is unlikely due to the induction of systemic TNF- $\alpha$ . Interestingly, systemic induction of IL-6 was detected following *Pg* infection. It has been shown that inhibition of IL-6 receptor directly blocks osteoclast formation in vitro and in vivo.<sup>42</sup> In addition, IL-6 has been reported to stimulate MDSC in multiple cancers<sup>43,44</sup> and hepatitis B infection.<sup>45</sup> Mechanisms responsible for promoting IL-6-dependent accumulation of myeloid cells involves the suppression of suppressor of cytokine signaling 3 (SOCS3)<sup>46</sup> and the activation of signal transducer of activation

transcription 3 (Stat3).<sup>47,48</sup> Interestingly, *Pg* has been shown to inhibit SOCS3 and increase Stat3 activation.<sup>49</sup> Therefore, it is possible that systemic induction of IL-6 following *Pg* infection may be involved in the expansion of CD11b<sup>+</sup>c-fms<sup>+</sup> cells observed in the present study. Current studies are evaluating this possibility.

It has been demonstrated that hematopoietic stem cells express various TLRs and that TLR-mediated signals skew hematopoiesis to myeloid lineage.<sup>50</sup> Therefore, we anticipated that TLR signaling is involved in *Pg*-induced expansion of osteoclast precursors. Using MyD88<sup>-/-</sup> mice, we showed that MyD88 is involved in *Pg*-mediated expansion of CD11b<sup>+</sup>c-fms<sup>+</sup> cells in bone marrow and spleen. Furthermore, MyD88 also played a role in *Pg*-mediated inflammation and bone loss, suggesting that MyD88 regulates *Pg*-induced bone loss, at least partially, through the regulation of osteoclast precursors. Our results are in agreement with several in vitro and in vivo studies reporting a MyD88-dependent expansion and activation of MDSC by TLR2 or TLR4 signaling.<sup>47,51-53</sup> However, we have previously shown that *Pg*-induced expansion of MDSC was MyD88-independent in a 14-day subcutaneous infection model.<sup>31</sup> Others have shown that MyD88 is essential for the immunosuppressive function of MDSC, but not essential for their induction.<sup>54</sup> In addition, reduced MDSC frequency and inhibited immunosuppressive effects by different TLR ligands have been reported.<sup>55,56</sup> On the other hand, a critical role of MyD88 in the regulation of inflammation and bone loss following infection with *Pg* or other pathogens has been reported,<sup>57-59</sup> which is in agreement with our current findings. However, it has been shown that although MyD88 is required for bacterial clearance, *Pg*-induced inflammatory responses and bone loss are MyD88-independent.<sup>38,60</sup> Hence, it is likely that the differences in the results of these studies can be explained by the nature, dose, and/or duration of the infection, as well as by the specifics of the microenvironment, thus influencing the participation of compensatory mechanisms involving signaling via different molecules.<sup>31</sup> Delineating the involvement of MyD88 in regulating *Pg*-mediated regulation of osteoclast precursors is important for further pursuing the involvement of TLR downstream molecules in *Pg*-induced expansion of osteoclast precursors, as well as the cross talk between TLR and RANK signaling in regulating inflammation and bone loss during periodontal infection.

In the present study, we show that CD11b<sup>+</sup>c-fms<sup>+</sup> cells composed the majority of monocytic MDSC, and were able to suppress OVA-driven antigen-specific CD4<sup>+</sup> T-cell proliferation, highlighting an important functional cross talk between osteoclast precursors and the host immune response. Invasion of host by pathogens leads to the activation of the innate immune system, after which an adaptive immune response develops to eradicate the infection and establish memory. On the other hand, the immune system also develops a variety of counter-regulatory mechanisms, including regulatory T cells, regulatory B cells, tolerogenic DC, and MDSC, which are intended to achieve a balance between maximizing clearance of infectious pathogens and minimizing collateral tissue damage.<sup>61,62</sup> However, many pathogens including *Pg* can evolve mechanisms to hijack these immune regulatory mechanisms to ensure their long-term survival by preventing immune clearance.<sup>63,64</sup> It is believed that immune activation and suppression coexist in

infectious diseases, and immunosuppressive activities are more profound in the setting of chronic infections or chronic inflammation than in acute conditions.<sup>65,66</sup> Under chronic conditions, some bacteria can induce immunosuppressive activity following immune activation, thus blocking antigen-specific immune responses that are essential for clearing pathogens, and contributing to the chronicity of the infection by enabling bacterial persistence. Indeed, evidence exists that sustained exposure to *Pg* impairs T-cell function, resulting in the attenuation of a chronically activated immune response.<sup>64</sup> However, the underlying mechanisms involved in T-cell suppression by *Pg* are not fully understood. Based on our results, it is possible that osteoclast precursors, as a subpopulation of MDSC, are involved in damping CD4<sup>+</sup> T-cell responses following immune activation, thus contributing to the persistence of infection and maintenance of chronic inflammation.

In our studies, no increase in osteoclastogenesis or bone loss was seen in long bones following calvarial infection. Elevated osteoclast differentiation and bone loss occurred only at the calvarial infection site where there were significantly elevated levels of pro-osteoclastogenic molecules including RANKL, IL-1 $\beta$ , and TNF- $\alpha$ . These results further suggest that the expanded osteoclast precursors induced by *Pg* infection are not lineage-determined. They function as immune regulatory cells in the circulation and differentiate into osteoclasts at the local pro-osteoclastogenic environment. However, given the increasing evidence suggesting systemic inflammatory bone loss diseases, such as rheumatoid arthritis, as a risk factor for chronic periodontitis and vice versa,<sup>67,68</sup> it is not unreasonable to hypothesize that increased osteoclast precursors are involved in the association of chronic periodontitis and various inflammatory bone loss diseases.<sup>69</sup> Indeed, patients with active erosive arthritis have a marked increase in the frequency of peripheral blood CD11b<sup>+</sup> osteoclast precursors.<sup>70</sup> These cells might promote alveolar bone loss when they reach inflamed periodontal tissues. Conversely, increased frequency and function of osteoclast precursors in peripheral blood mononuclear cells of patients with chronic periodontitis<sup>69,71,72</sup> might lead to periarticular erosions and systemic osteoporosis in both its emergence and progress if periarticular and systemic inflammation persists.

Collectively, our findings support a model whereby *Pg* infection increases a pool of precursor cells that can be shunted toward osteoclast formation at the local infection/inflammation sites, while at the same time dampening host immune responses, which is beneficial for the persistence of infection and maintenance of the characteristic chronic nature of periodontitis. It is likely that this enhanced dual function of osteoclast precursors is critical for the pathological consequences of *Pg* infection in vivo. Understanding the nature, function, and regulation of osteoclast precursors will be important for understanding host susceptibility to periodontal bone loss and should help reveal novel diagnostic markers and therapeutic strategies to prevent bone loss associated with infection and inflammation.

#### ACKNOWLEDGEMENTS

We thank Gregory Harber for his technical assistance. This work was supported by the National Institute of Dental and Craniofacial

Research (NIDCR) grants DE022401 (to P. Z.) and DE026465 (to P. Z.). Z. L. was supported by NIDCR training grant T90 DE022736. The University of Alabama at Birmingham Comprehensive Flow Cytometry Core is supported by the National Institutes of Health (NIH) grants P30AI27667 and P30AR048311; the Small Animal Phenotyping Core is supported by the NIH grants P30DK056336, P30DK079626, and P30AG050886A.

## CONFLICT OF INTEREST

All authors state that they have no conflict of interests.

## ORCID

Ping Zhang  <https://orcid.org/0000-0002-4585-9893>

## REFERENCES

- Jacome-Galarza CE, Percin GI, Muller JT, et al. Developmental origin, functional maintenance and genetic rescue of osteoclasts. *Nature*. 2019;568:541-545.
- Cochran DL. Inflammation and bone loss in periodontal disease. *J Periodontol*. 2008;79:1569-1576.
- Goldring SR, Gravalles EM. Pathogenesis of bone erosions in rheumatoid arthritis. *Curr Opin Rheumatol*. 2000;12:195-199.
- Xing L, Schwarz EM, Boyce BF. Osteoclast precursors, RANKL/RANK, and immunology. *Immunol Rev*. 2005;208:19-29.
- Asagiri M, Takayanagi H. The molecular understanding of osteoclast differentiation. *Bone*. 2007;40:251-264.
- Teitelbaum SL, Ross FP. Genetic regulation of osteoclast development and function. *Nat Rev Genet*. 2003;4:638-649.
- Lamont RJ, Jenkinson HF. Life below the gum line: pathogenic mechanisms of *Porphyromonas gingivalis*. *Microbiol Mol Biol Rev*. 1998;62:1244-1263.
- Van Dyke TE, Lester MA, Shapira L. The role of the host response in periodontal disease: implications for future treatment strategies. *J Periodontol*. 1993;64:792-806.
- Takeuchi Y, Umeda M, Sakamoto M, Benno Y, Huang Y, Ishikawa I. *Treponema socranskii*, *Treponema denticola*, and *Porphyromonas gingivalis* are associated with severity of periodontal tissue destruction. *J Periodontol*. 2001;72:1354-1363.
- Griffen AL, Lyond SR, Becker MR, Moeschberger ML, Leys EJ. *Porphyromonas gingivalis* strain variability and periodontitis. *J Clin Microbiol*. 1999;37:4028-4033.
- Brown LJ, Loe H. Prevalence, extent, severity and progression of periodontal disease. *Periodontol* 2000. 1993;2:57-71.
- Delaney JE, Keels MA. Pediatric oral pathology. *Pediatr Oral Health*. 2000;47:1125-1147.
- Lin X, Han X, Kawai T, Taubman MA. Antibody to receptor activator of NF- $\kappa$ B ligand ameliorates T cell-mediated periodontal bone resorption. *Infect Immun*. 2011;79:911-917.
- Teng YT, Nguyen H, Gao X, et al. Functional human T cell immunity and osteoprotegerin ligand control alveolar bone destruction in periodontal infection. *J Clin Invest*. 2000;106:59-67.
- Kawai T, Matsuyama T, Hosokawa Y, et al. B and T lymphocytes are the primary sources of RANKL in the bone resorptive lesion of periodontal disease. *Am J Pathol*. 2006;169:987-998.
- Chen Z, Su L, Xu Q, et al. IL-1R/TLR2 through MyD88 divergently modulates osteoclastogenesis through regulation of nuclear factor of activated T cells c1 (NFATc1) and B lymphocyte-induced maturation protein 1 (Blimp1). *J Biol Chem*. 2015;290:30163-30174.
- Jules J, Feng X. In vitro investigation of the roles of the proinflammatory cytokines tumor necrosis factor-alpha and interleukin-1 in murine osteoclastogenesis. *Methods Mol Biol*. 2014;1155:109-123.
- Graves D. Cytokines that promote periodontal tissue destruction. *J Periodontol*. 2008;79:1585-1591.
- Zhang P, Liu J, Xu Q, et al. TLR2-dependent modulation of osteoclastogenesis by *Porphyromonas gingivalis* through differential induction of NFATc1 and NF- $\kappa$ B. *J Biol Chem*. 2011;286:24159-24169.
- Robertson JM, Jensen PE, Evavold BD. DO11.10 and OT-II T cells recognize a C-terminal ovalbumin 323-339 epitope. *J Immunol*. 2000;164:4706-4712.
- Graves DT, Fine D, Teng YT, Van Dyke TE, Hajishgeghallian G. The use of rodent models to investigate host-bacteria interactions related to periodontal diseases. *J Clin Periodontol*. 2008;35:89-105.
- Yao Z, Li P, Zhang Q, et al. Tumor necrosis factor-alpha increases circulating osteoclast precursor numbers by promoting their proliferation and differentiation in the bone marrow through up-regulation of c-Fms expression. *J Biol Chem*. 2006;281:11846-11855.
- Li P, Schwartz EM, O'Keefe RJ, et al. Systemic tumor necrosis factor alpha mediates an increase in peripheral CD11b<sup>high</sup> osteoclast precursors in tumor necrosis factor alpha-transgenic mice. *Arthritis Rheum*. 2004;50:265-276.
- Chellaiah MA. Regulation of actin ring formation by rho GTPases in osteoclasts. *J Biol Chem*. 2005;280:32930-32943.
- Jacquin C, Gran DE, Lee SK, Lorenzo JA, Aguila HL. Identification of multiple osteoclast precursor populations in murine bone marrow. *J Bone Miner Res*. 2006;21:67-77.
- Feng X. RANKing intracellular signaling in osteoclasts. *IUBMB Life*. 2005;57:389-395.
- Muto A, Mizoguchi T, Udagawa N, et al. Lineage-committed osteoclast precursors circulate in blood and settle down into bone. *J Bone Miner Res*. 2011;26:2978-2990.
- Mizoguchi T, Muto A, Udagawa N, et al. Identification of cell cycle-arrested quiescent osteoclast precursors in vivo. *J Cell Biol*. 2009;184:541-554.
- van Genderachter JA, Beschin A, De Baetselier P, Raes G. Myeloid-derived suppressor cells in parasitic infection. *Eur J Immunol*. 2010;40:2976-2985.
- Ezernitchi AV, Vaknin I, Cohen-Daniel L, et al. TCR  $\zeta$  down-regulation under chronic inflammation is mediated by myeloid suppressor cells differentially distributed between various lymphatic organs. *J Immunol*. 2006;177:4763-4772.
- Su L, Xu Q, Zhang P, Michalek SM, Katz J. Phenotype and function of myeloid-derived suppressor cells induced by *Porphyromonas gingivalis* infection. *Infect Immun*. 2017;85:e00213-7.
- Akira S, Takeda K. Toll-like receptor signaling. *Nat Rev*. 2004;4:499-511.
- Darveau RP, Pham TT, Lemley K, et al. *Porphyromonas gingivalis* lipopolysaccharide contains multiple lipid A species that functionally interact with toll-like receptor 2 and 4. *Infect Immun*. 2004;72:5041-5051.
- Gaddis DE, Michalek SM, Katz J. Requirement of TLR4 and CD14 in dendritic cell activation by hemagglutinin B from *Porphyromonas gingivalis*. *Mol Immunol*. 2009;46:2493-2504.
- Burns E, Bachrach G, Shapira L, Nussbaum G. Cutting edge: TLR2 is required for the innate response to *Porphyromonas gingivalis*: activation leads to bacterial persistence and TLR2 deficiency attenuates induced alveolar bone resorption. *J Immunol*. 2006;177:8296-8300.
- Costalonga M, Batas L, Reich BJ. Effects of Toll-like receptor 4 on *Porphyromonas gingivalis*-induced bone loss in mice. *J Period Res*. 2008;44:537-542.
- Hou L, Sasaki H, Stashenko P. Toll-like receptor 4-deficient mice have reduced bone destruction following mixed anaerobic infection. *Infect Immun*. 2000;68:4681-4687.
- Burns E, Eliyahu T, Uematsu S, Akira S, Nussbaum G. TLR2-mediated inflammatory response to *Porphyromonas gingivalis* is MyD88 independent, whereas MyD88 is required to clear infection. *J Immunol*. 2010;184:1455-1462.

39. Shi C, Pamer EG. Monocyte recruitment during infection and inflammation. *Nat Rev Immunol*. 2011;11:762-774.
40. Atkin MB, Kostakis P, Vincent C, et al. RANK expression as a cell surface marker of human osteoclast precursors in peripheral blood, bone marrow, and giant cell tumors of bone. *J Bone Miner Res*. 2006;21:1339-1349.
41. Liu J, Wang S, Zhang P, Said-Al-Naief N, Michalek SM, Feng X. Molecular mechanism of bifunctional role of lipopolysaccharide (LPS) in osteoclastogenesis. *J Biol Chem*. 2009;284:12512-12523.
42. Axmann R, Bohm C, Kronke G, Zwerina J, Smolen J, Schett G. Inhibition of interleukin-6 receptor directly blocks osteoclast formation in vitro and in vivo. *Arthritis Rheum*. 2009;60:2747-2756.
43. Mundy-Bosse BL, Young GS, Bauer T, et al. Distinct myeloid suppressor cells subsets correlate with plasma IL-6 and IL-10 and reduced interferon-alpha signaling in CD4+ T cells from patients with GI malignancy. *Cancer Immunol Immunother*. 2011;60:1269-1279.
44. Tsukamoto H, Nishikata R, Senju S, Nishimura Y. Myeloid-derived suppressor cells attenuate TH1 development through IL-6 production to promote tumor progression. *Cancer Immunol Res*. 2013;1:64-76.
45. Fang Z, Li J, Yu X, et al. Polarization of monocytic myeloid-derived suppressor cells by hepatitis B surface antigen is mediated via ERK/IL-6/STAT3 signaling feedback and restrains the activation of T cells in chronic hepatitis B virus infection. *J Immunol*. 2015;195:4873-4883.
46. Jiang M, Chen J, Zhang W, et al. Interleukin-6 Trans-signaling pathway promotes immunosuppressive myeloid-derived suppressor cells via suppression of suppressor of cytokine signaling 3 in breast cancer. *Front Immunol*. 2017;8:1840.
47. Ost M, Singh A, Peschel A, Mehling R, Nikolaus R, Hartl D. Myeloid-derived suppressor cells in bacterial infections. *Front Cell Infect Microbio*. 2016;6:1-9.
48. Sawant A, Deshane J, Jules J, et al. Myeloid-derived suppressor cells function as novel osteoclast progenitors enhancing bone loss in breast cancer. *Cancer Res*. 2013;73:672-682.
49. Moffatt CE, Lamont RJ. *Porphyromonas gingivalis* induction of microRNA-203 expression controls suppressor of cytokine signaling 3 in gingival epithelial cells. *Infect Immun*. 2011;79:2632-2637.
50. Esplin BL, Shimazu T, Welner RS, et al. Chronic exposure to a TLR ligand injures hematopoietic stem cells. *J Immunol*. 2011;186:5367-5375.
51. Maruyama A, Shime H, Takeda Y, Azuma M, Matsumoto M, Seya T. Pam2 lipopeptides systemically increase myeloid-derived suppressor cells through TLR2 signaling. *Biochem Biophys Res Commun*. 2015;457:445-450.
52. Ray A, Chakraborty K, Ray P. Immunosuppressive MDSCs induced by TLR signaling during infection and role in resolution of inflammation. *Front Cell Infect Microbiol*. 2013;3:52.
53. Delano MJ, Scumpia PO, Weinstein JS, et al. MyD88-dependent expansion of an immature GR-1(+)/CD11b(+) population induces T cell suppression and Th2 polarization in sepsis. *J Exp Med*. 2007;204:1463-1474.
54. Hong EH, Chang SY, Lee BR, et al. Blockade of MyD88 signaling induces antitumor effects by skewing the immunosuppressive function of myeloid-derived suppressor cells. *Int J Cancer*. 2013;132:2839-2848.
55. Shirota Y, Shirota H, LKlinman DM. . Intratumoral injection of CpG oligonucleotides induces the differentiation and reduces the immunosuppressive activity of myeloid-derived suppressor cells. *J Immunol*. 2012;188:1592-1599.
56. Zhao BG, Vasilakos JP, Tross D, Smirnov D, Klinman DM. Combination therapy targeting toll like receptors 7, 8, and 9 eliminates large established tumors. *J Immunother Cancer*. 2014;2:12.
57. Madeira MF, Queiroz-Junior CM, Cisalpino D, et al. MyD88 is essential for alveolar bone loss induced by *Aggregatibacter actinomycetemcomitans* lipopolysaccharide in mice. *Mol Oral Microbiol*. 2013;38:415-424.
58. Putman NE, Fulbright LE, Curry JM, Ford CA, Petronglo JR, Hendrix AS. MyD88 and IL-1R signaling drive antibacterial immunity and osteoclast-driven bone loss during *Staphylococcus aureus* osteomyelitis. *PLoS Pathog*. 2019;15:e1007744.
59. Kassem A, Henning P, Lundberg P, Souza PPC, Lindholm C, Lerner UH. *Porphyromonas gingivalis* stimulates bone resorption by enhancing RANKL through activation of Toll-like receptor 2 in osteoblasts. *J Biol Chem*. 2015;290:20147-20158.
60. Makkawi H, Hoch S, Burns E, Hosur K, Hajishengallis G, Kirschning CJ, Nussbaum G. *Porphyromonas gingivalis* stimulates TLR2-PI3K signaling to escape immune clearance and induce bone resorption independently of MyD88. *Front Cell Infect Microbiol*. 2017;7:359.
61. Kondo Y, Shimosegawa T. Significant roles of regulatory T cells and myeloid derived suppressor cells in Hepatitis B virus persistent infection and Hepatitis B virus-related HCCs. *Int J Mol Sci*. 2015;16:3307-3322.
62. Lindau D, Gielen P, Kroesen M, Wesseling P, Adema GJ. The immunosuppressive tumor network: myeloid-derived suppressor cells, regulatory T cells and natural killer T cells. *Immunology*. 2013;138:105-115.
63. Tebartz C, Horst SA, Sparwasser T, et al. A major role for myeloid-derived suppressor cells and a minor role for regulatory T cells in immunosuppression during *Staphylococcus aureus* infection. *J Immunol*. 2015;194:1100-1111.
64. Bronstein-Sitton N, Cohen-Daniel L, Vaknin I, et al. Sustained exposure to bacterial antigen induces interferon- $\gamma$ -dependent T cell receptor  $\zeta$  down-regulation and impaired T cell function. *Nat Immunol*. 2003;4:957-964.
65. Dai J, Gazzar ME, Li GY, Moorman JP, Yao Z. Myeloid-derived suppressor cells: paradoxical roles in infection and immunity. *J Innate Immun*. 2015;7:116-126.
66. Brudecki L, Ferguson DA, McCall CE, El Gazzar M. Myeloid-derived suppressor cells evolve during sepsis and can enhance or attenuate the systemic inflammatory response. *Infect Immun*. 2012;80:2026-2034.
67. Bingham CO III, Moni M. Periodontal disease and rheumatoid arthritis: the evidence accumulates for complex pathobiologic interactions. *Curr Opin Rheumatol*. 2013;25:345-353.
68. Rosenstein ED, Kushner LJ, Kramer N. Rheumatoid arthritis and periodontal disease: A rheumatologist's perspective. *Curr Oral Health Rep*. 2015;2:9-19.
69. de Vries TJ, el Bakkali I, Kamradt T, Schett G, Jansen IDC, D'Amelio P. What are the peripheral blood determinants for increased osteoclast formation in the various inflammatory diseases associated with bone loss. *Front Immunol*. 2019;10: Article 505.
70. Ritchlin CT, Haas-Smith SA, Li P, Hicks DG, Schwarz EM. Mechanisms of TNF- $\alpha$ - and RANKL-mediated osteoclastogenesis and bone resorption in psoriatic arthritis. *J Clin Invest*. 2003;111:821-831.
71. Tjoa STS, de Vrles TJ, LKelder A, Loos BG, Everts V. . Formation of osteoclast-like cells from peripheral blood of periodontitis patients occurs without supplementation of macrophage colony-stimulating factor. *J Clin Periodontol*. 2008;35:568-575.
72. Herrera BS, Bastos AS, Coimbra LS, et al. Peripheral blood mononuclear phagocytes from patients with chronic periodontitis are primed for osteoclast formation. *J Periodontol*. 2014;85:e72-e81.

**How to cite this article:** Cai X, Li Z, Zhao Y, et al. Enhanced dual function of osteoclast precursors following calvarial *Porphyromonas gingivalis* infection. *J Periodont Res*. 2020;55:410-425. <https://doi.org/10.1111/jre.12725>